Journal of Alloys and Compounds 500 (2010) 200–205

Contents lists available at ScienceDirect

Journal of Alloys and Compounds

journal homepage: www.elsevier.com/locate/jallcom

Study on the dehydrogenation kinetics and thermodynamics of $Ca(BH_4)_2$

Jianfeng Mao[a], Zaiping Guo[a,b,*], Chung Kiak Poh[a], Abbas Ranjbar[a], Yanhui Guo[c], Xuebin Yu[c,a,**], Huakun Liu[a]

[a] Institute for Superconducting and Electronic Materials, University of Wollongong, NSW 2522, Australia
[b] School of Mechanical, Materials & Mechatronics Engineering, University of Wollongong, NSW 2522, Australia
[c] Department of Materials Science, Fudan University, Shanghai 200433, China

ARTICLE INFO

Article history:
Received 23 February 2010
Received in revised form 22 March 2010
Accepted 31 March 2010
Available online 7 April 2010

Keywords:
Hydrogen storage
$Ca(BH_4)_2$
Kinetics
Thermodynamics

ABSTRACT

$Ca(BH_4)_2$ is a promising hydrogen storage material due to its high gravimetric hydrogen density of 11.5 wt%. In this work, the dehydrogenation kinetics and thermodynamics of $Ca(BH_4)_2$ were systematically investigated by differential thermal analysis (DTA), thermal analysis mass spectrometry (TA/MS), temperature-programmed desorption (TPD), X-ray diffraction (XRD) and pressure, composition, and temperature (PCT) measurements. DTA, TA/MS, TPD and XRD results indicate that the dehydrogenation process of $Ca(BH_4)_2$ is a two-step reaction. The dehydriding reaction of $Ca(BH_4)_2$ starts at approximately 320 °C, and about 9.6% of hydrogen is desorbed through the two-step reaction. The apparent activation energy (E_a) of about 225.37 and 280.51 kJ/mol for the first-step and second-step dehydrogenation, respectively, were determined by Kissinger's method. The activation energy for the first-step dehydrogenation was further confirmed by the Arrhenius equation. As a result of in-depth kinetic investigations, a geometrical contraction-controlled kinetic mechanism has been identified for the first-step dehydrogenation by analyzing isothermal hydrogen desorption curves with a linear plot method. Finally, the thermodynamic parameters for the dehydrogenation are estimated based on the results of the PCT measurements: enthalpy of reaction $\Delta H = 87$ kJ/mol-H_2, and entropy of reaction $\Delta S = 158$ J/K mol-H_2. The relatively high activation energy and change in enthalpy indicate that a kinetic and thermodynamic barrier needs to be overcome for $Ca(BH_4)_2$ to be suitable as a hydrogen storage material for mobile applications.

1. Introduction

New types of clean energy sources, such as wind, solar, and hydroelectric, have attracted intense attention, due to the limited supply of fossil oil and the environmental issues from burning carbon-based fuel. In this context, hydrogen is a potential major alternative energy carrier. However, there still need to be global efforts aimed at developing advanced hydrogen storage materials with high gravimetric and volumetric density. These need to have rapid, energy efficient (de)hydriding reactions under mild conditions [1,2]. Since Bogdanovic and Schwickardi discovered that Ti-catalysed $NaAlH_4$ could store H_2 reversibly under moderate conditions in 1997 [3], lightweight hydrogen storage materials such as alanates, amides, and borohydrides have attracted growing attention and have been explored intensively, due to their high gravimetric densities of hydrogen for hydrogen storage [4–10].

$LiBH_4$, due to its high capacity (18.5 wt%), was first investigated as a candidate for hydrogen storage materials in the family of metal borohydrides, $M(BH_4)_n$ (where n indicates the valence of metal M). However, its high dehydriding temperature (>400 °C) and rigorous conditions of reversibility (600 °C, 150 bar) are big obstacles to hydrogen storage applications [11]. Various investigation and preparation methods, such as structural analysis, study of dehydrogenation/rehydrogenation behaviors, mechanical milling, catalyst doping, etc., have been undertaken to overcome the kinetic and thermodynamics limitations [12–23]. However, even the enhanced $LiBH_4$ is still unable to meet the requirements for mobile application. Recently, Nakamori et al. found by first-principle calculations that the dehydrogenation temperature of $M(BH_4)_n$ decreases with an increase in the value of the electronegativity of M [24]. From this point of view, $Ca(BH_4)_2$ may have superior dehydrogenation/rehydrogenation kinetics and thermodynamics compared to $LiBH_4$.

As $Ca(BH_4)_2$ has a high theoretical hydrogen capacity of 11.5 wt%, it is considered as a prospective material for hydrogen storage. Recently, the structure and dehydriding behavior of $Ca(BH_4)_2$ have been explored both theoretically and experimen-

* Corresponding author at: Institute for Superconducting and Electronic Materials, University of Wollongong, NSW 2522, Australia. Tel.: +61 2 4221 5225; fax: +61 2 4221 5731.
** Corresponding author at: Department of Materials Science, Fudan University, Shanghai 200433, China.
E-mail addresses: zguo@uow.edu.au (Z. Guo), yuxuebin@fudan.edu.cn (X. Yu).

0925-8388/$ – see front matter © 2010 Elsevier B.V. All rights reserved.
doi:10.1016/j.jallcom.2010.03.242

tally [25–30]. The most likely decomposition routes of $Ca(BH_4)_2$ are assumed from density functional theory (DFT) calculations to be as described in the following equations [31]:

$$Ca(BH_4)_2 \rightarrow 2/3CaH_2 + 1/3CaB_6 + 10/3H_2$$

$$\Delta H_{DFT} = -40.6\,kJ/mol\text{-}H_2,\ \Delta S_{DFT} = 109.3\,J/K\,mol\text{-}H_2,$$
$$\text{yield} = 9.6\,wt\%\,H_2 \quad (1)$$

where ΔH_{DFT} is the change in enthalpy calculated from density functional theory and ΔS_{DFT} is the calculated entropy of the reaction.

$$Ca(BH_4)_2 \rightarrow CaH_2 + 2B + 3H_2$$

$$\Delta H_{DFT} = -57.3\,kJ/mol\text{-}H_2,\ \Delta S_{DFT} = 105.7\,J/K\,mol\text{-}H,$$
$$\text{yield} = 8.7\,wt\%\,H_2 \quad (2)$$

However, according to reported experimental results, the following dehydrogenation path of $Ca(BH_4)_2$ has been suggested [30,31]:

$$Ca(BH_4)_2 \rightarrow CaH_2 + \text{intermediate compound} \rightarrow CaH_2 + CaB_6 + H_2 \quad (3)$$

More recently, Riktor et al. [32] identified the unknown intermediate compound to be CaB_2H_x by high-resolution synchrotron radiation powder X-ray diffraction and suggested that the x most probably equals 2. In contrast, Wang et al. [33] suggested the intermediate compound to be $CaB_{12}H_{12}$ by experiment and first-principle calculations.

However, at present, the detailed dehydrogenation kinetics and thermodynamics of $Ca(BH_4)_2$ are still unclear, which has considerable importance for understanding the nature of the hydrogen storage properties. In addition, according to the DFT prediction, the hydrogen desorption of Eq. (1) should occur at temperatures around 98 °C at 1.0 atm hydrogen pressure. Unfortunately, a detectable rate of hydrogen desorption was experimentally attained only at temperatures above 200 °C, indicating the presence of a relatively high kinetic and thermodynamic barrier for this reaction.

In this work, the thermal decomposition process of $Ca(BH_4)_2$ was studied by differential thermal analysis (DTA), thermal analysis mass spectrometry (TA/MS), temperature-programmed desorption (TPD), and X-ray diffraction (XRD) measurements. The results indicate that the dehydrogenation process of $Ca(BH_4)_2$ is a two-step reaction. The apparent activation energy was further calculated and discussed. For the dehydrogenation kinetic mechanism, isothermal hydrogen desorption measurements were conducted on the first-step decomposition of $Ca(BH_4)_2$, and the curves attained were analyzed with a linear plot method. The dehydrogenation process of $Ca(BH_4)_2$ was found to be a geometrical contraction-controlled kinetic mechanism. In addition, the thermodynamic parameters of enthalpy change and entropy change were calculated and discussed.

2. Experimental

The $Ca(BH_4)_2$ was purchased from Sigma–Aldrich and used without any further purification. X-ray diffraction (XRD) data were acquired at room temperature on a Rigaku D/max 2200PC X-ray diffractometer with Cu Kα radiation at 40 kV and 30 mA from 10° to 90° (2θ) with a scan rate of 4°/min. Samples were mounted onto a 1-mm depth glass board in an Ar-filled glove box and sealed with an amorphous membrane in order to avoid oxidation during the XRD measurement. All samples were handled in an Ar-filled glove box (MBRAUN), in which both H_2O and O_2 concentrations were kept below 1 ppm.

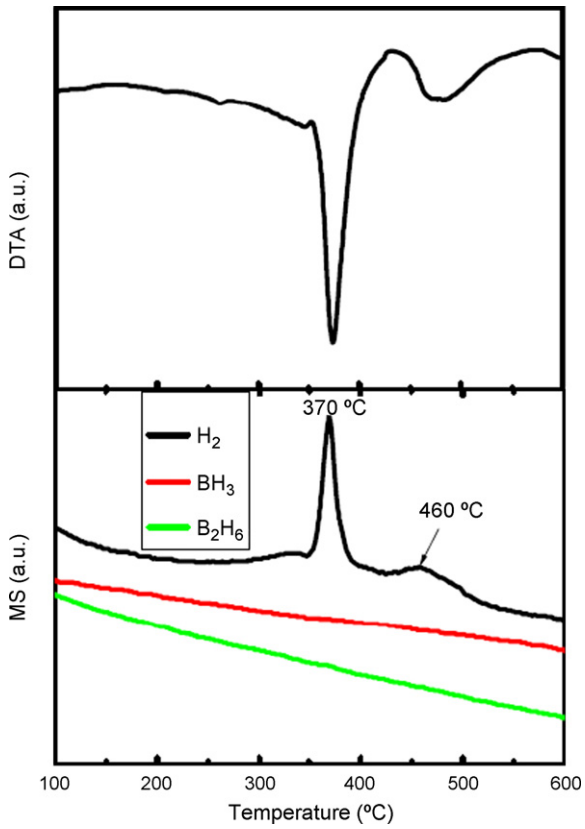

Fig. 1. Thermal analysis mass spectrometry (TA/MS) and differential thermal analysis (DTA) curves of $Ca(BH_4)_2$.

Differential thermal analysis (DTA) measurements of the sample were performed on a STA 449C instrument connected to a mass spectrometer (QMS 403) for thermal analysis mass spectrometry (TA/MS) measurements, using a heating rate of 10 °C min^{-1} under 1 atm argon atmosphere.

TPD curves were determined by volumetric methods with a Sieverts-type Gas Reaction Controller (GRC), a product of Advanced Materials Corporation (USA). Both isothermal and non-isothermal measurements were made. In the non-isothermal experiment, the sample was gradually heated to the desired temperature at an average ramp of 1, 3, 5 and 10 °C/min, respectively (initially in vacuum). For isothermal desorption kinetic measurements, the sample was quickly heated to and then kept at the given temperature. The pressure change in the reactor with time was recorded over the temperature range of 300–360 °C. Quantities of hydrogen desorbed were determined by the pressure changes in the reactor by means of the ideal gas law calculation. Pressure–composition–temperature (PCT) isotherm measurements were carried out in the same Sieverts-type instrument. A ~200 mg sample was loaded into a sample holder having a thermocouple well-located in the center of the sample. Temperatures and pressures of the sample and the gas reservoirs were monitored and recorded by the GrcLV-LabVIEW-based control program software during sorption process.

3. Results and discussion

The hydrogen desorption of the $Ca(BH_4)_2$ was studied by means of DTA and TA/MS, as shown in Fig. 1. One sharp and one broad endothermic peak with small shoulders are observed between 200 and 600 °C in the DTA curve. Correspondingly, at least two overlapping peaks are confirmed in the TA/MS curve of $Ca(BH_4)_2$. As seen from the TA/MS results, two peaks of hydrogen evolution are obvious in the temperature range of 300–500 °C, with the peak temperatures at around 370 and 460 °C, respectively. The DTA and TA/MS results indicate that the dehydrogenation process of $Ca(BH_4)_2$ is a two-step reaction, which suggests the presence of an intermediate compound, similar to the case of $LiBH_4$ [12]. So far, $Ca(BH_4)_2$ has been reported to desorb hydrogen in accordance with Eq. (3), and an intermediate compound has also been suggested [31,32].

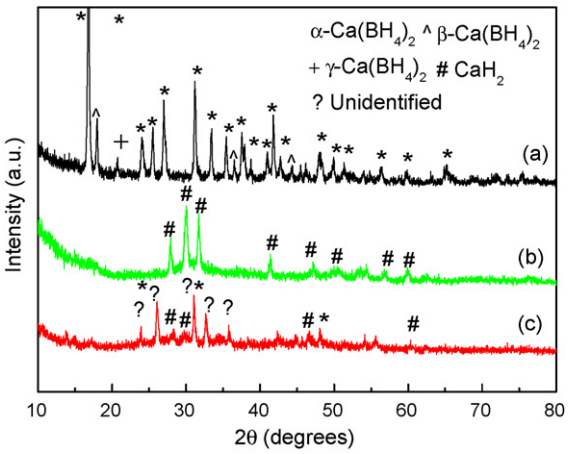

Fig. 2. XRD patterns of $Ca(BH_4)_2$ before (a) and after dehydrogenation at (b) 500 °C and (c) 320 °C.

To better understand the decomposition mechanism, XRD diffraction analysis was carried out on the as-received $Ca(BH_4)_2$, as well as on the dehydrogenation products. Fig. 2 shows the XRD patterns of the as-received $Ca(BH_4)_2$ before and after dehydrogenation at 320 and 500 °C, respectively. The as-received $Ca(BH_4)_2$ is a mixture of α-, β-, and γ-$Ca(BH_4)_2$, but is mainly α-$Ca(BH_4)_2$. After dehydrogenation to 320 °C, most $Ca(BH_4)_2$ peaks were absent, and new compounds, corresponding to an intermediate compound and some CaH_2 were observed. The peak positions of the intermediate compound agree well with previous reports [29,31]. However, there is still some disagreement about the intermediate phase. Ozolins et al. [34] predicted the possible intermediate $CaB_{12}H_{12}$ by theoretical first-principle methods. Wang et al. [33] suggested the intermediate compound to be $CaB_{12}H_{12}$ by experiment and first-principle calculations. However, Riktor et al. [32] have proposed CaB_2H_x as the unknown intermediate compound by high-resolution synchrotron radiation powder X-ray diffraction and suggested that the x most probably equals 2. The different results show that the decomposition scheme for $Ca(BH_4)_2$ may highly depend on the experimental conditions. After dehydrogenation at 500 °C, the intermediate disappeared and the main phase is CaH_2. The results of XRD also indicate that the dehydrogenation process of $Ca(BH_4)_2$ is a two-step reaction.

The quantity of hydrogen desorbed from each reaction step was further measured by the volumes of hydrogen gathered, starting from vacuum. Fig. 3(a) shows the TPD results for $Ca(BH_4)_2$ at variable heating rates. Hydrogen desorption starts at about 320 °C with two evident desorption steps, comparing well with the TA/MS results. Hydrogen desorption curves were shifted to higher temperatures as the heating rate increased from 1 to 10 °C/min, as expected. In the case of 1 °C/min, the two dehydrogenation steps take place one after the other in the temperature ranges of 310–350 and 350–500 °C to desorb 5.66 and 4.23 wt% hydrogen, respectively. In the case of 10 °C/min, the two dehydrogenation steps take place one after the other to desorb 5.96 and 3.88 wt% hydrogen, respectively, in the temperature ranges of 310–380 and 380–500 °C. The hydrogen desorption rates of $Ca(BH_4)_2$ were calculated from the hydrogen desorption curves by plotting the hydrogen desorption capacity against time (Fig. 3(b)). Two maximum desorption rates were clearly observed in all the cases of different heating rates, corresponding to the two-step dehydrogenation of $Ca(BH_4)_2$ and comparing well with the TA/MS and TPD results. The temperatures for the first maximum desorption rate are 335, 348, 357 and 366 °C; 411, 427, 437 and 443 °C are observed for the second maximum desorption rate, corresponding to the heating rates of 1, 3, 5, and 10 °C/min, respectively. The discrepancy in the peak temperatures

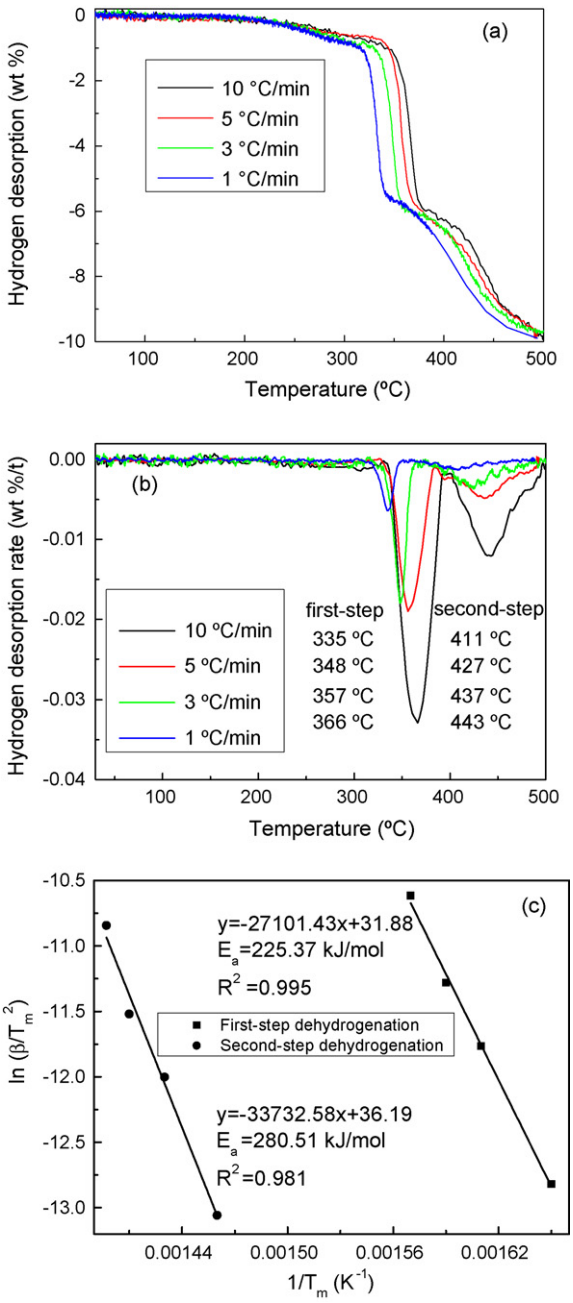

Fig. 3. TPD (temperature-programmed desorption) (a) and hydrogen desorption rate (b) curves of $Ca(BH_4)_2$ at various heating rates; and the Kissinger's plot (c).

originates from the particular temperature-hydrogen desorption experiments, as the TA/MS and DTA were carried out in hydrogen atmosphere and in inert gas, respectively.

The activation energy (E_a), for the hydrogen desorption mechanism of $Ca(BH_4)_2$ was obtained from TPD measurements at different heating rates by Kissinger's method [35]:

$$\ln\left(\frac{\beta}{T_m^2}\right) = -\frac{E_a}{RT} \quad (4)$$

where β is the heating rate in °C/min, T_m is the absolute temperature for the maximum desorption rate, and R is the gas constant. In the present study, T_m was extracted from the hydrogen desorption rate curves at variable heating rates, as shown in Fig. 3(c). The T_m shifts to higher values when the heating rate increases from 1 to 10 °C/min. The plot of $\ln(\beta/T_m^2)$ versus $1/T_m$ is also a straight line,

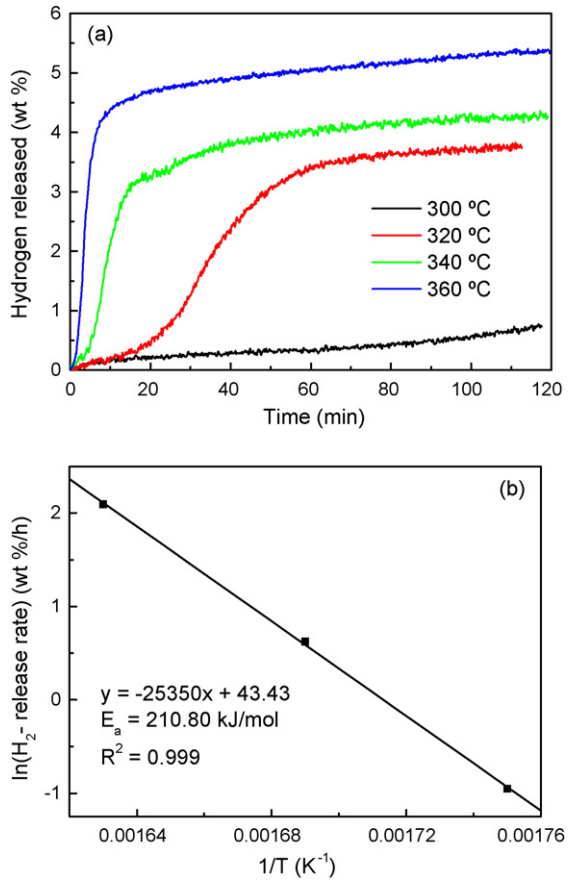

Fig. 4. Isothermal hydrogen desorption curves (a) of $Ca(BH_4)_2$ at 300–360 °C and (b) the Arrhenius plot.

as shown in Fig. 3(c). From the slope of the straight line, the activation energy E_a was determined to be approximately 225.37 and 280.51 kJ/mol for the first-step and second-step dehydrogenation reactions of $Ca(BH_4)_2$, respectively.

For further investigating the mechanism of the reaction kinetics, isothermal dehydrogenation experiments were carried out at 300–360 °C. Fig. 4(a) shows the isothermal dehydrogenation curves of $Ca(BH_4)_2$ at 300, 320, 340, and 360 °C. As the operating temperature increased, the dehydrogenation rate distinctly speeded up. At 300 °C, only 0.77 wt% hydrogen was released at 120 min. In contrast, 3.8, 4.3, and 5.37 wt% hydrogen can be released at 120 min at 320, 340, and 360 °C, respectively. The isothermal dehydrogenation curves at 320, 340 and 360 °C exhibit the typical sigmoidal shape, with a short induction period, followed by an acceleration period for dehydrogenation, and finally a decaying period. It takes 4 min to desorb 50% of the hydrogen from the first-step desorption at 360 °C, but 14 and 49 min are required to desorb the same amount of hydrogen at 340 and 320 °C, respectively.

To further investigate the rate constant, the activation energy (E_a) of the first-step dehydrogenation of $Ca(BH_4)_2$ was further evaluated by the Arrhenius equation [36,37]: rate (wt%/h) = $k_o \exp(-E_a/RT)$, where k_0 is a constant. As shown in Fig. 4(b), this is achieved by plotting ln(H_2 release rate) versus $1/T$. The apparent activation energy (E_a) for H_2 release was determined to be 210.80 kJ/mol, which is very close to the value that was determined by Kissinger's method.

In the literature, several solid-state reaction mechanism models have been proposed, including the nucleation, the geometrical contraction, the diffusion, and the reaction order models, based on the different geometries of the particles and the different driving forces, which are listed in Table 1 [38–44]. To identify the solid-state reaction mechanism, a Jones method [45] was used to select a proper model which involves all essential chemical steps. In the Jones method, the theoretical value $(t/t_{0.5})_{theo}$ is plotted against the experimental data $(t/t_{0.5})_{exp}$ of different rate equations to produce a linear plot, where t is the time and $t_{0.5}$ means half the time for the reaction to be completed. The value of the linear slope of an acceptable model should be very close to 1. The relationship of $(t/t_{0.5})_{exp}$ versus $(t/t_{0.5})_{theo}$ for the dehydrogenation of $Ca(BH_4)_2$ at 360 °C is listed above the graphs in Fig. 5. It can be seen that the $(t/t_{0.5})_{exp}$ value plotted against the $(t/t_{0.5})_{theo}$ value of the R2 model exhibits a good linear relationship, with a slope close to 1. This finding indicates that the hydrogen desorption reaction of $Ca(BH_4)_2$ correlates closely to the geometrical contraction-controlled kinetic mechanism represented by the R2 model. This model assumes that nucleation occurs rapidly on the surface of the crystal. The rate of degradation is controlled by the progress of the resulting reaction interface toward the center of the crystal. Dehydration of calcium oxalate monohydrate has been shown to follow a geometrical contraction model [46–48].

Table 1
Kinetic models examined in the isothermal dehydrogenation curves of $Ca(BH_4)_2$ at 360 °C.

Symbol	Model	Integral $f(\alpha)$ form	R^2
D1	1D diffusion	α^2	1.469
D2	2D diffusion	$\alpha + (1-\alpha)\ln(1-\alpha)$	1.663
D3	3D diffusion (Jander equation)	$[1-(1-\alpha)^{1/3}]^2$	1.935
D4	3D diffusion (Ginstling–Braunshteinn equation)	$1-(2\alpha/3)-(1-\alpha)^{2/3}$	1.728
F1	First-order reaction	$-\ln(1-\alpha)$	1.173
R2	Contracting area	$1-(1-\alpha)^{1/2}$	1.003
R3	Contracting volume	$1-(1-\alpha)^{1/3}$	1.059
A2	Avarami–Erofeev	$[-\ln(1-\alpha)]^{1/2}$	0.657
A3	Avarami–Erofeev	$[-\ln(1-\alpha)]^{1/3}$	0.461

The isothermal dehydriding properties of $Ca(BH_4)_2$ in hydrogen atmosphere at 629, 647, 662, and 686 K from investigation by using PCT (pressure, composition and temperature) measurements are shown in Fig. 6. The measurements at 629 K were started at a pressure of 30 bar, and the other measurements at higher temperature were started at a higher pressure (60 bar) because the plateau pressures were expected to be at much higher pressures than 30 bar. At 629 K, the desorbed amount of hydrogen is 6.24 wt%. As the operating temperature increased, the desorbed amount of hydrogen distinctly increased. The desorbed amount of hydrogen is 6.59, 6.95 and 7.71 wt% at 647, 662, and 686 K, respectively. The

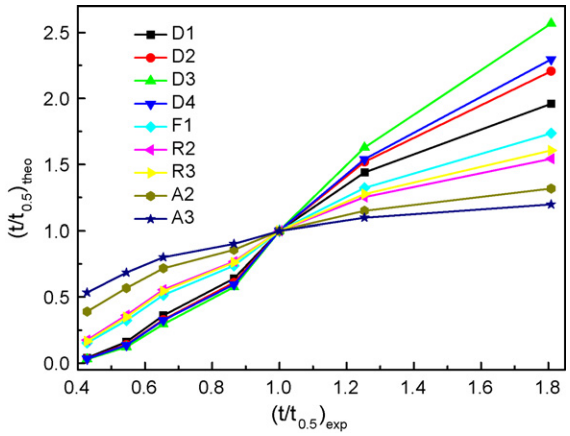

Fig. 5. $(t/t_{0.5})_{theo}$ vs. $(t/t_{0.5})_{exp}$ of $Ca(BH_4)_2$ dehydrogenated at 360 °C for various solid-state reaction equations.

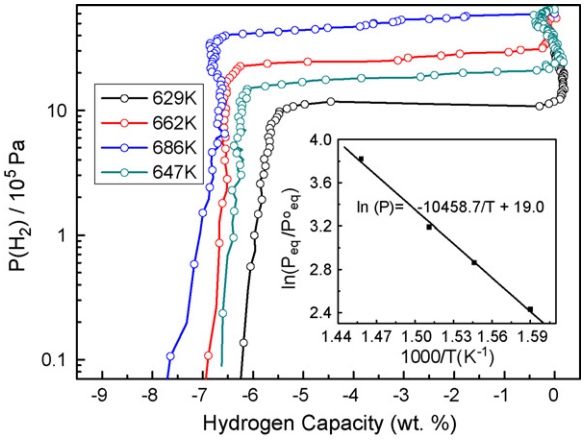

Fig. 6. Pressure–composition–temperature (PCT) curves of $Ca(BH_4)_2$ measured at 629, 647, 662, and 686 K. The inset shows the van't Hoff plot for $Ca(BH_4)_2$.

amount of hydrogen desorption for $Ca(BH_4)_2$ observed from the PCT measurements is larger than that indicated by the temperature-program desorption results; this can be attributed to the different experimental conditions (temperature and hydrogen pressure) or the low kinetics of the dehydriding reaction in the programmed experimental time. One plateau is observed at 629 K at a hydrogen pressure of 11.5 bar, whereas two plateaus are observed for 647, 662, and 686 K within the hydrogen pressure range of 15–60 bar, in agreement with the two-step dehydriding reaction from $Ca(BH_4)_2$ to CaH_2, as shown by the TPD curves (Fig. 3(a)). Therefore, the isothermal dehydriding reaction results also strongly indicate the formation of some intermediate compound during the dehydriding process from $Ca(BH_4)_2$ to CaH_2, as indicated by the TPD results.

It is well-known that the thermodynamic parameters, the desorption enthalpy change (ΔH) and the entropy change (ΔS), of a metal hydride can be calculated from the temperature-dependent equilibrium pressure (P) in the van't Hoff equation [49]:

$$\ln\left(\frac{P_{eq}}{P_o}\right) = \frac{\Delta H}{RT} - \frac{\Delta S}{R} \quad (5)$$

where P_o is the standard pressure (1.01325 bar), T is the absolute temperature and R is the gas constant. The slope of the straight line is proportional to ΔH and the axis intercept is proportional to ΔS. The van't Hoff plot for the dehydriding reaction from $Ca(BH_4)_2$ to CaH_2 is shown in the inset to Fig. 6. As discussed above, there are two plateaus in the PCT curves at 647, 662, and 686 K, and it is difficult to exactly distinguish these two regions. Therefore, the enthalpy and entropy are roughly estimated; the equilibrium pressure P_{eq} at each temperature is designated as the pressure value at the median of dehydrogenation capacity. Based on the van't Hoff plot, the enthalpy and entropy for the dehydriding reaction from $Ca(BH_4)_2$ to CaH_2 are estimated to be $\Delta H = 87$ kJ/mol-H_2 and $\Delta S = 158$ J/K mol-H_2, respectively. These values are higher than the standard enthalpies and entropies of reaction assumed from density functional theory (DFT) calculations [31]. Because the dehydrogenation reaction of $Ca(BH_4)_2$ was a two-step reaction and the assumed enthalpy and entropy by density functional theory (DFT) calculations is based on one-step reaction. It cannot be excluded that the equilibrium is not fully reached although the fitted points are well-located on straight lines for the extrapolation to equilibrium and on the van't Hoff plot. More details on the kinetics and thermodynamics, as well as the structures of intermediate compound are in progress.

4. Conclusions

The dehydrogenation kinetics and thermodynamics of $Ca(BH_4)_2$ were systematically investigated. The dehydriding reaction of $Ca(BH_4)_2$ starts at approximately 320 °C, and approximately 9.6% of the hydrogen is desorbed up to 500 °C in a two-step reaction. Kinetic investigations indicated that a relatively high kinetic barrier needs to be surmounted for hydrogen desorption from $Ca(BH_4)_2$, with an activation energy of approximately 225.37 and 280.51 kJ/mol for the first step and the second step, respectively. A geometrical contraction-controlled kinetic mechanism was identified for the first-step dehydrogenation by analyzing isothermal hydrogen desorption curves by a linear plot method. Based on the results of the PCT measurements, the enthalpy change and entropy change were estimated to be 87 kJ/mol-H_2 and 158 J/K mol-H_2, respectively, by using the van't Hoff equation.

Acknowledgments

This work was partially supported by Australian Research Council (ARC) Discovery projects (DP0771193, DP0878661) and the CSIRO Flagship Program, as well as the Hi-Tech Research and Development Program of China (grant no. 2007AA05Z107), the Shanghai Leading Academic Discipline Project (grant no. B113), the Shanghai Rising-Star Program (grant no. 05QMX1463), and the Shanghai Pujiang Program (grant no. 08PJ14014).

References

[1] U.S. National Academy of Sciences, The Hydrogen Economy: Opportunities, Cost, Barriers and R&D Needs, The National Academies Press, Washington, DC, 2004.
[2] L. Schlapbach, A. Züttel, Nature 414 (2001) 353–358.
[3] B. Bogdanović, M. Schwickardi, J. Alloys Compd. 1 (1997) 253–254.
[4] J. Chen, N. Kuriyama, Q. Xu, H.T. Takeshita, T. Sakai, J. Phys. Chem. B 105 (2001) 11214–11220.
[5] G. Meisner, G. Tibbetts, F. Pinkerton, C. Olk, M. Balog, J. Alloys Compd. 337 (2002) 254–263.
[6] P. Chen, Z.T. Xiong, J.Z. Luo, J.Y. Lin, K.L. Tan, Nature 420 (2002) 302–304.
[7] H.Y. Leng, T. Ichikawa, S. Hino, N. Hanada, S. Isobe, H. Fujii, J. Phys. Chem. B 108 (2004) 8763–8765.
[8] A. Züttel, S. Rentsch, P. Fischer, P. Wenger, P. Sudan, Ph. Mauron, Ch. Emmenegger, J. Alloys Compd. 356–357 (2003) 515.
[9] K. Chłopek, C. Frommen, A. Léon, O. Zabara, M. Fichtner, J. Mater. Chem. 17 (2007) 3496–3503.
[10] H.W. Li, K. Kikuchi, Y. Nakamori, N. Ohba, K. Miwa, S. Towata, S. Orimo, Acta Mater. 56 (2008) 1342–1347.
[11] A. Züttel, P. Wenger, S. Rentsch, P. Sudan, Ph. Mauron, Ch. Emmenegger, J. Power Sources 118 (2003) 1–7.
[12] S.J. Hwang, R.C. Bowman, J.W. Reiter, Rijssenbeek, G.L. Soloveichik, J.C. Zhao, H. Kabbour, Ch.C. Ahn, J. Phys. Chem. C 112 (2008) 3164–3169.
[13] Z.Z. Fang, X.D. Kang, P. Wang, H.M. Cheng, J. Phys. Chem. C 112 (2008) 17023–17029.
[14] M. Au, A. Jurgensen, J. Phys. Chem. B 110 (2006) 7062–7067.
[15] M. Au, A. Jurgensen, J. Phys. Chem. B 110 (2006) 26482–26487.
[16] M. Au, A. Jurgensen, W.A. Spencer, D.L. Anton, F.E. Pinkerton, S.J. Hwang, C. Kim, R.C. Bowman, J. Phys. Chem. C 112 (2008) 18661–18671.
[17] F.E. Pinkerton, M. Meyer, G. Meisner, M. Balogh, J. Vajo, J. Phys. Chem. C 111 (2007) 12881–12885.
[18] A. Gross, J. Vajo, S.L. Van Atta, G. Olson, J. Phys. Chem. C 112 (2008) 5651–5657.
[19] J. Vajo, S. Skeith, F. Mertens, J. Phys. Chem. C 109 (2005) 3719–3722.
[20] X.B. Yu, D.M. Grant, G.S. Walker, Chem. Commun. 37 (2006) 3906–3908.
[21] X.B. Yu, Z. Wu, W.R. Chen, X.L. Li, B.C. Weng, T.S. Huang, Appl. Phys. Lett. 90 (2007) 034106.
[22] X.B. Yu, D.M. Grant, G.S. Walker, J. Phys. Chem. C 112 (2008) 11059–11062.
[23] J. Yang, A. Sudik, C. Wolverton, J. Phys. Chem. C 111 (2007) 19134–19140.
[24] Y. Nakamori, K. Miwa, A. Ninomiya, H. Li, N. Ohba, S. Towata, A. Züttel, S. Orimo, Phys. Rev. B 74 (2006) 045126.
[25] E. Rönnebro, E.H. Majzoub, J. Phys. Chem. B 111 (2007) 12045–12047.
[26] Y. Filinchuk, E. Rönnebro, D. Chandra, Acta Mater. 57 (2009) 732–738.
[27] E.H. Majzoub, E. Rönnebro, J. Phys. Chem. C 113 (2009) 3352–3358.
[28] K. Miwa, M. Aoki, T. Noritake, N. Ohba, Y. Nakamori, S. Towata, A. Züttel, S. Orimo, Phys. Rev. B 74 (2006) 155122.
[29] M. Aoki, K. Miwa, T. Noritake, N. Ohba, M. Matsumoto, H.W. Li, Y. Nakamori, S. Towata, S. Orimo, Appl. Phys. A 92 (2008) 601–605.
[30] J.H. Kim, S.A. Jin, J.H. Shim, Y.W. Cho, J. Alloys Compd. 461 (2008) L20–L22.

[31] Y. Kim, D. Reed, Y.S. Lee, J.Y. Lee, J.H. Shim, D. Book, Y.W. Cho, J. Phys. Chem. C 113 (2009) 5865–5871.
[32] M.D. Riktor, M.H. Sørby, K. Chłopek, M. Fichtner, B.C. Hauback, J. Mater. Chem. 19 (2009) 2754–2759.
[33] L.L. Wang, D.D. Graham, I.M. Robertson, D.D. Johnson, J. Phys. Chem. C 113 (2009) 20088–20096.
[34] V. Ozolins, E.H. Majzoub, C. Wolverton, J. Am. Chem. Soc. 131 (2009) 230–237.
[35] H.E. Kissinger, Anal. Chem. 29 (1957) 1702–1706.
[36] J.W. Christian, The Theory of Transformations in Metals and Alloys, 2nd ed., Pergamon, New York, 1975.
[37] X.D. Kang, Z.Z. Fang, L.Y. Kong, H.M. Cheng, X.D. Yao, G.Q. Lu, P. Wang, Adv. Mater. 29 (2008) 2756–2759.
[38] A.M. Ginstling, Brounshteın, J. Appl. Chem. USSR (Engl. Transl.) 23 (1950) 1327–1338.
[39] G. Valensi, Compt. Rend. 202 (1936) 309–312.
[40] R.E. Carter, J. Chem. Phys. 34 (1961) 2010–2015.
[41] J.B. Holt, I.B. Culter, M.E. Wadsworth, J. Am. Ceram. Soc. 45 (1962) 133–136.
[42] W.Z. Jander, Anorg. Allgem. Chem. 163 (1927) 1–30.
[43] M. Avrami, J. Chem. Phys. 7 (1939) 1103–1112.
[44] B.V. Erofe'ev, Compt. Rend. Acad. Sci. URSS 52 (1946) 511–514.
[45] L.F. Jones, D. Dollimore, T. Nicklim, Therm. Acta 13 (1975) 240–245.
[46] G. Chunxiu, S. Yufang, C. Donghua, J. Therm. Anal. Calorim. 76 (2004) 203.
[47] L. Liqing, C. Donghua, J. Therm. Anal. Calorim. 78 (2004) 283.
[48] Z.M. Gao, I. Amasaki, M. Nakada, Thermochim. Acta 385 (2002) 95.
[49] G. Sandrock, J. Alloys Compd. 293–295 (1999) 877–888.